Image segmentation,
bilateral filter, Canny-Deriche edge detector,
micro tomography, porous materials

Mateusz BUCZKOWSKI[1], Khalid SAEED[1,2]

A MULTISTEP APPROACH FOR MICRO TOMOGRAPHY OBTAINED MEDICAL IMAGE SEGMENTATION

This paper presents a multistep approach for segmentation of micro tomography images. Various images of porous structures were studied. Proper segmentation of that images is necessary to create 3D models of these structures. The introduced algorithm concerns finding the proper way of image filtering before the use of Canny-Deriche edge detection to obtain the best possible segmentation.

1. Introduction

Images were acquired using micro tomography technique (μCT). That technique allows to study nondestructive internal structures imaging of any object. X-ray tube generates x-ray electromagnetic radiation which penetrates through the studied sample. Attenuation of x-rays intensity is registered at the opposite side of the sample by two-dimensional detector. Value of x-ray intensity registered in each pixel of the detector depend on materials property across beam path. Captured image is called “projection”. After acquiring one projection sample is rotated by small angle and another projection is captured. Few hundreds or few thousands of projections are acquired. Software reconstruct 3D object from set of projections using one of existing methods. For example filtered back projection method based on Radon transform theorem [8]. The reconstructed object is represented by 3D matrix of voxels. To separate material phases every 2D slice of that matrix should be segmented. That allows to create 3D model of studied sample and calculate volumes of each individual phases. The X-ray measurements presented in this paper were obtained using ”nanotom 180N” device produced by GE Sensing & Inspection Technologies phoenix X-ray Gmbh equipped with nanofocus X-ray tube with maximum 180kV voltage. The tomograms were registered on Hamamatsu 2300x2300 pixel detector and reconstruction of measured objects was done using of proprietary GE software datosX ver. 2.1.0 with Feldkamp algorithm for cone beam X-ray CT [4].

[1] Faculty of Physics and Applied Computer Science AGH University of Science and Technology, Krakow, Poland
[2] Faculty of Computer Science, Bialystok University of Technology, Bialystok, Poland

2. USED METHODS

2.1. BILATERAL FILTER

Bilateral filter is a smoothing technique which allows to remove unwanted textures, noise and insignificant details but preserves large edges without blurring at the same time. Simple Gaussian filter blurs unwanted details but edges as weel. Bilateral filter is based on Gaussian convolution. Gaussian filtering is based on weighted average of the adjacent pixels intensities in the given neighbourhood Blur increases with increasing size of the filter convolution mask. Weights are decreasing with increasing spatial distance from the central pixel according to Gaussian distribution:

$$G[I]_p = \frac{1}{W_{pG}} \sum_{q \in S} G_\sigma(||p-q||) I_q, \tag{1}$$

where: $G_\sigma(x)$ is Gaussian convolution kernel given by (2), S is the spatial domain, W_{pG} is sum of all weights, I is intensity of pixel, $||p-q||$ is the Euclidean distance between the central pixel p and another pixel q form the given neighbourhood. Neighbourhood size is given by σ.

Larger sigma results in more flat distribution, lower sigma describes more steep distribution. Main disadvantage of Gaussian filtering is edge blurring which do not let to preserve edges.

$$G_\sigma(x) = \frac{1}{2\pi\sigma} exp\left(-\frac{x^2}{2\sigma^2}\right) \tag{2}$$

Bilateral filter is defined as:

$$B[I]_p = \frac{1}{W_{pB}} \sum_{q \in S} G_{\sigma_s}(||p-q||) G_{\sigma_r}(||I_p - I_q||) I_q, \tag{3}$$

where:

$$W_{pB} = \sum_{q \in S} G_{\sigma_s}(||p-q||) G_{\sigma_r}(||I_p - I_q||). \tag{4}$$

Only pixels close in space and intensity range are considered. Gaussian kernel used in spatial domain (G_{σ_s}) decreases weights with increasing distance and acts like simple Gaussian filter. Gaussian kernel used in intensity range domain (G_{σ_r}) decreases weights with increasing intensity differences. Combination of both kernels in spatial and intensity range domain gives bilateral filter capability of smoothing image and preserve edges at the same time [7]. These properties are very useful for smoothing μCT images studied in this paper where noise level is high and edges are weak.

2.2. CANNY-DERICHE EDGE DETECTOR

Canny formulated three most important criteria for effective edge detection:

- Good detection - low probability of failing to detect existing true edges and low probability of false edge detection
- Good localization - found edges should be as close as possible to the true edges
- One response to one edge - multiply responses to one real edge should not appear, one edge should create only one response

Canny combined these criteria into one optimal operator and found that it is approximately the first derivative of Gaussian [2, 3] - see (5).

$$f(x) = -\frac{x}{\sigma^2} e^{-\frac{x^2}{2} \cdot \sigma^2}. \tag{5}$$

In 1987 Deriche modified Canny approach to construct optimal edge detector [3]. He proposed edge detector with impulse response given by:

$$f(x) = k \cdot e^{-\alpha \cdot |x|} \sin \omega x \tag{6}$$

and second version when ω tends to 0:

$$g(x) = k \cdot x e^{-\alpha \cdot |x|} \tag{7}$$

Performance of that approach is significantly better than the first derivative of a Gaussian presented by Canny. At the beginig calculations of magnitude and gradient direction are performed. Then non-maximal suppression allows to select the single maximum point across the width of an edge. That step thin edges. After that hysteresis thresholding is performed to get the final output. Hysteresis thresholding using two thresholds divides pixels into three groups. Pixels below low threshold are removed, pixels above high threshold are retained. Pixels which intensities are placed between low and high threshold are retained only if connected to another pixel above high threshold [2, 3].

3. Parameters adjust

Various parameters were adjusted:

- Bilateral filter: Mask size, intensity range, spatial sigma, intensity sigma
- Canny-Deriche edge detector: alpha, high threshold, low threshold
- Too short edges removing: threshold

The procedure was applied to smaller fragments of original images [1]. The first studied image contained small objects, the second bigger objects.

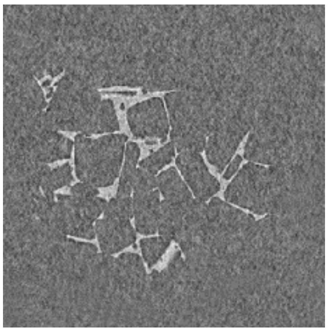

(a)

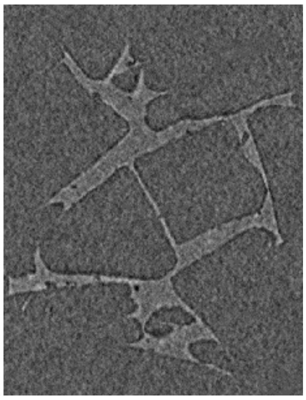

(b)

Fig. 1: Studied images fragments in original resolution: containing small objects (a) and big objects (b).

Objects edges were marked by hand to create benchmark images Fig. 2. Parameters were adjusted by comparison results of edge detection with tested parameters to benchmark image accordingly to equation:

$$Q = \frac{N_p - N_n}{N_0} \cdot 100\% \tag{8}$$

where: Q- detection quality (result closer to 100% is better), N_p *- number of positively detected pixels,* N_n *- number of false detected pixels.* N_0 *- number of all edge pixels in the benchmark image.*

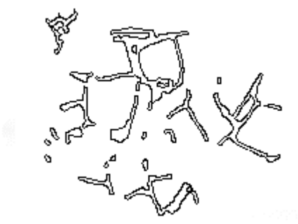

(a)

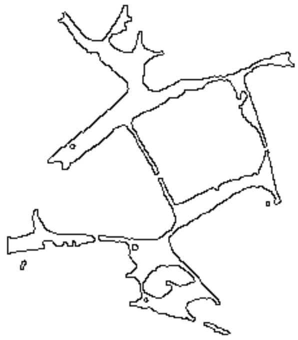

(b)

Fig. 2: Benchmark images in original resolution: image containing small objects (a), image containing big objects (b).

All results were sorted by edge detection quality based on equation 8. Parameters set with highest detection quality were used to process original full size images. For Fig. 1A best parameters set reached 89% detection quality score, for Fig. 1B 86%. If parameters adjust uses image fragments, high and low threshold parameters might need some manual correction because gradient map of full image and image fragment could have slightly different intensity values due to gradient magnitude normalisation. Problem does not exist if full image is used for parameters adjust but in that approach if large images with huge amount of objects are processed it could be time-consuming to mark edges manually to create benchmark image.

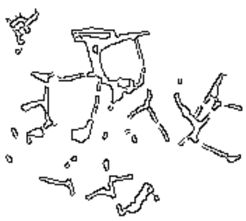

(a)

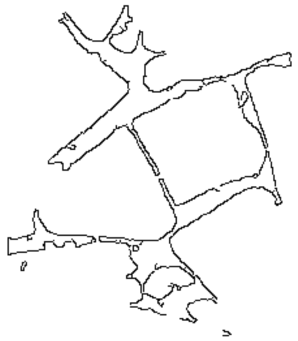

(b)

Fig. 3: Test images processed with best parameters set: image containing small objects (a), image containing big objects (b).

Images were divided into two groups: containing small objects and containing big objects. To assign new image to one of the classes algorithm find edges by using default parameters values chosen to give acceptable results on images from both classes. All edge pixels which distance from another is smaller than chosen threshold are considered as one object. Algorithm compute number of pixels for all objects what reflects object size. Its assumed that object with more pixels is bigger than object containing less pixels. For tested image mean value of pixels per object were computed. Based on that value and chosen threshold, images could be classified as containing small objects or containing big objects. For example first tested image (Fig. 1A) have mean object size value 86 and it is considered as containing small object and second (Fig. 1B) with mean object size value equals to 199 is considered as containing big objects. In this case threshold could be set around 143. Depend on studied images collection, input images set could be divided into more groups. Parameters could be adjusted analogically for each group. That approach allows to automatically process set of hundreds images representing slices of object studied using micro tomography. Parameters are adjusted using only fragment of one slice.

4. The proposed methodology

First image is converted to grayscale if needed (Fig. 4). Next histogram normalisation is applied (Fig. 5). Smoothing steep involves bilateral filter (Fig. 6). Edge detection is achieved by using Canny-Deriche edge detector. First gradient map is calculated (Fig. 7). Then non-maximum suppression is applied to thin edges (Fig. 8). Finally Hysteresis thresholding is applied to remove false edges (Fig. 9). Last step removes too short edges (Fig. 10).

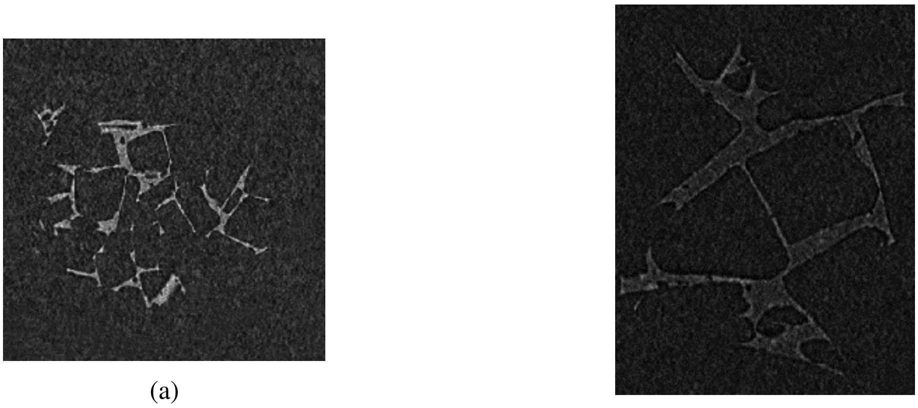

(a) (b)

Fig. 4: Images after conversion to greyscale: image containing small objects (a), image containing big objects (b).

Grayscale conversion is performed to make sure that processed image type is greyscale because algorithm is adapted to work with graysclae images.

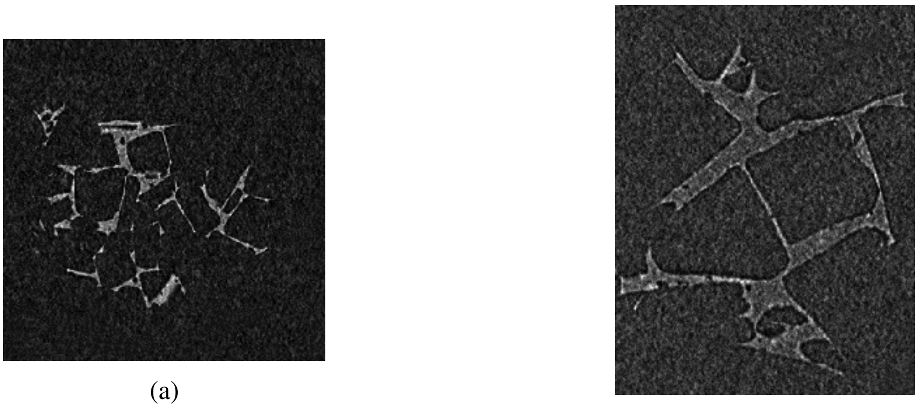

(a) (b)

Fig. 5: Image after histogram normalisation: image containing small objects (a), image containing big objects (b).

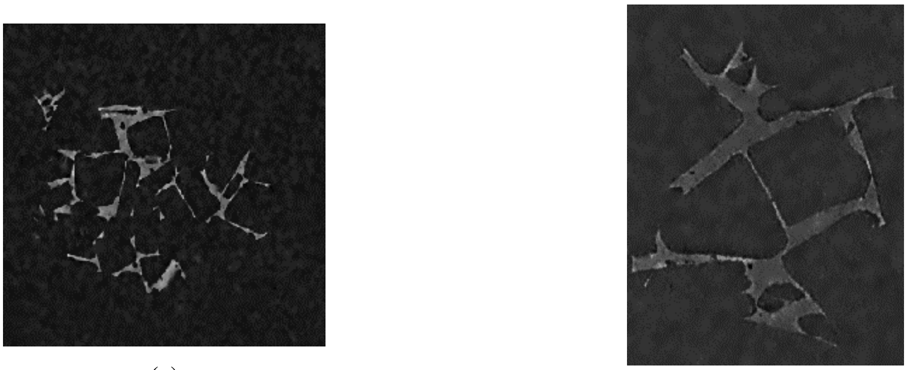

(a) (b)

Fig. 6: Image after use of bilateral filter: image containing small objects (a), image containing big objects (b)

Bilateral filter was used because it performs better than approach based on classical Gaussian filter or median filter. In future works it is planned to try other denoising methods like Anisotropic denoising for example.

(a) (b)

Fig. 7: Canny-Deriche edge detection gradient magnitude: image containing small objects (a), image containing big objects (b).

(a) (b)

Fig. 8: Canny-Deriche edge detection non-maximum suppression: image containing small objects (a), image containing big objects (b).

Non-maximum suppression allows to thin edges. One pixel width edges are necessary to obtain good edge localisation after thresholding.

(a) (b)

Fig. 9: Canny-Deriche edge detection result: image containing small objects (a), image containing big objects (b).

(a) (b)

Fig. 10: Images after removal of too short edges: image containing small objects (a), image containing big objects (b).

Removal of too short edges allows to remove false detected edges resulting from noise which remained after bilateral filtering.

5. Experimental results and Interpretation

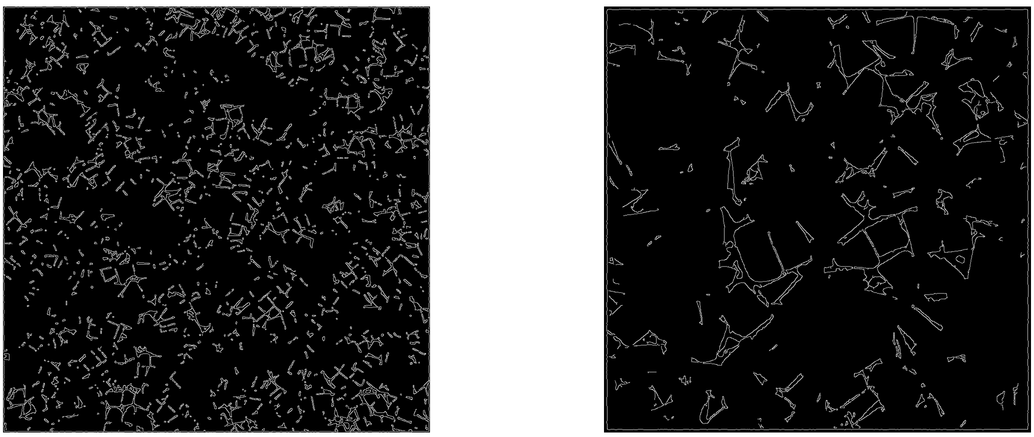

(a) (b)

Fig. 11: Algorithm output for full size test images: image containing small objects (a), image containing big objects (b).

The algorithm produces very small amount of false edges detected only those very weak and hard to differ from background are not detected. Performance of some other segmentation methods on that kind of images was shown earlier - see [1]. Using Bilateral filtering prior to Canny-Deriche edge detector results better edge detection than Canny-Deriche algorithm itself. Some objects are not fully segmented. Some small gaps in edges occurred. Parameters of Canny-Deriche edge detector and bilateral filter were semi-automatic adjusted. We hope that the approach proposed after some modifications could give fully segmented images. Images could be partially segmented already by using similar approach as described in object size detection step. Presented method allows to treat weak contrast images giving good results of image segmentation.

ACKNOWLEDGEMENT

The research was partially supported by grant no. WFiIS 11.11.220.01/saeed, AGH University of Science and Technology in Krakow. Authors are indebted to professor Jacek Tarasiuk and his team for providing us with the input images to our algorithm.

BIBLIOGRAPHY

[1] BUCZKOWSKI M., SAEED K., TARASIUK J., WROSKI S., KOSIOR J., In: R. Chaki et al. (eds.), Applied Computation and Security Systems, Advances in Intelligent Systems and Computing 304, 2014.
[2] CANNY J., A computational approach to edge detection. Pattern Analysis and Machine Intelligence, IEEE Transactions on 6, 1986, pp. 679-698.
[3] DERICHE R., Using Canny's criteria to derive a recursively implemented optimal edge detector. International journal of computer vision 1.2, 1987, pp. 167-187.
[4] FELDKAMP LA, DAVIS LC, KRESS JW, Practical cone-beam algorithm. J Opt Soc Am, A6, 1984, pp. 612-9.
[5] HE LEI, ET AL, A comparative study of deformable contour methods on medical image segmentation. Image and Vision Computing 26.2, 2008, pp. 141-163.
[6] JAHNE B., Digital Image Processing: Concept, Algorithms, and Scientific Applications. Springer, 1997.
[7] PARIS S., KORNPROBST P., TUMBLIN J., DURAND F., Bilateral Filtering: Theory and Applications. Foundations and Trends in Computer Graphics and Vision, 2008, Vol. 4, No. 1, pp. 173.
[8] RADON J., Uber die Bestimmung von Funktionen durch ihre Integralwerte Langs Gewisser Mannigfaltigkeiten. Ber. Saechsische Akad. Wiss. 29, 1917, pp. 262.
[9] ROGOWSKA J., Overview and fundamentals of medical image segmentation. Handbook of medical imaging, Academic Press, Inc., 2000, pp. 69-85.
[10] SAEED K., ALBAKOOR M., Region Growing Based Segmentation Algorithm for Typewritten, and Handwritten Text Recognition. Applied Soft Computing, Elsevier Science Publishers, 2009, Vol. 9 , No. 2, pp. 608-617.
[11] SEZGIN M., SANKUR B., Survey over image thresholding techniques and quantitative performance evaluation, Journal of Electronic Imaging 13(1), 2004, pp. 146165.
[12] XU C., PHAM L. D., PRINCE J. L., , Image segmentation using deformable models. Handbook of medical imaging 2, 2000, pp. 129-174.
[13] VOLUME GRAPHICS GMBH, EDITOR, Reference Manual VGStudio Max Release 2.0; http://www.volumegraphics.com/en/products/vgstudio-max/ 8.10.2013